Turk J Phys
28 (2004) , 17 – 24.

Numerical Simulation of Soliton Pulse Propagation in Doped Optical Fibres by Finite-Difference Method

Adam USMAN[1], Junaidah OSMAN[2], David Reginald TILLEY[2]
[1]*Department of Physics, Federal University of Technology,*
PMB 2076, Yola, Adamawa State, NIGERIA
e-mail: aausman@yahoo.co.uk
[2]*School of Physics, Universiti Sains Malaysia, 11800 USM Penang, MALAYSIA*

Received 16.06.2003

Abstract

We report results of applications of explicit finite-difference schemes, viz. the combination of forward-difference and central-difference approximation schemes, to study a simulation of soliton pulse propagation in saturable optical fibres. The dynamic governing equation is the saturable nonlinear Schrödinger equation (SNLE). This equation thus far lacks analytical solution in the sense of the inverse scattering method, although an analytical solitary wave solution is available. We use the localized solution to generate data for simulations of fundamental and second order soliton pulse propagation. In addition, we check the numerical accuracy of the results by considering the physical significance of two conserved quantities which are properties of the governing equation.

Key Words: Soliton pulse, optical fibres, finite-difference, nonlinear Schrödinger equations.

1. Introduction

The optical soliton has undergone three decades of research, for its promising application to the future of telecommunication technology viz. future systems of global networks for information transmission [1–3]. An optical soliton, or soliton pulse, is a solitary wave which propagates through a nonlinear medium with constant velocity, undistorted profile, and conserved energy and momentum. Solitons arise from a balance between the inherent dispersion and nonlinear properties of optical fibres, characteristics which may be applied in communication systems and optical devices [4, 5].

To model soliton pulse propagation in optical fibres, dynamic equations known as nonlinear Schrödinger equations (NLSE's) are derived from Maxwell's equations via the slowly varying envelope approximation [6]. Optical fibre may be produced from pure or doped silica. Doped silica supports shorter pulse durations; and the pulse dynamics are described by either the cubic quintic nonlinear Schrödinger equation (CQNLSE) [7], or the saturable nonlinear Schrödinger equation (SNLSE) [6]. The well-known cubic nonlinear Schrödinger equation (CNLSE) [5, 8] models soliton propagation in pure (undoped) optical silica fibres.

The SNLSE may be classified into two forms, according to the saturating nonlinearity terms: denominating or exponential [9–11]. This report is concerned with the former. SNLSE with denominating nonlinearity terms has no exact solutions in the sense of the inverse scattering method (ISM), although analytical solitary wave solutions have been done [11]. However, analytical approximations using the variational method are

available [10]. The results show that the soliton amplitude is dependent on the saturation parameter of the fibre, and for certain values of this parameter there exist two possible soliton amplitudes. Numerical results using the pseudospectral method have confirmed the finding. The pseudospectral approach is usually the preferred choice in numerical work because of its computational speed. However, for the NLSE, this method does not satisfy some important conservation laws. Consequently, the validity of numerical results is not easily checked.

In this paper we present an alternative numerical approach to simulating the SNLSE, via the so-called explicit finite-difference method introduced by [12]. The method is simpler and it provides similar accuracy to the pseudospectral method. The most important advantage of this technique is that it provides an easy way of checking the numerical results through calculating the conserved quantities of the SNLSE.

In section two, we formulate how the problem is to be solved numerically. Section three is concerned with the numerical schemes for (i) the localized profiles and (ii) dynamic pulse profiles. Numerical results are discussed in section four. Conclusions are presented in section five.

2. Problem Formulation

The dimensionless form of the SNLSE can be written [6, 9, 10] as

$$i\frac{\partial q}{\partial \xi} - \delta\frac{\partial^2 q}{\partial s^2} + \frac{|q|^2 q}{1+\gamma|q|^2} = 0, \tag{1}$$

where $\xi \equiv z/L_D$ is the dimensionless distance along which the pulse propagates, z being the real displacement, and $L_D \equiv \tau_o^2/|\beta_2|$ is the dispersion length, with β_2 denoting the dispersion parameter; $s \equiv (t - z/v_g)/\tau_o$ is the dimensionless modulated time, t is the real time, v_g is the group velocity and τ_o is the pulse duration; $q(\xi, s) \equiv A(\xi, s)/A_o$ is the complex dimensionless propagating field amplitude; $A(\xi, s)$, in units of volts, is the actual slowly varying complex envelope field amplitude and $A_o \equiv \sqrt{2P_o/n_0\varepsilon_o c})$ is the input field at $\xi = z = 0$ with P_o, n_o, ε_o and c respectively denoting input power, linear refraction index of the fibre, free space permittivity and speed of light; and γ is the saturation parameter of the fibre. For soliton pulse propagation in the anomalous dispersion regime, $\delta = -1/2$; and $\delta = +1/2$ for normal dispersion propagation. We consider the former here.

2.1. Stationary profiles

The starting point is to look for the fundamental dimensionless localized solution of Equation (1) wherein $\delta = -1/2$, i.e. a bright soliton pulse propagation in the anomalous regime. The usual ansatz is thus given [6, 10] by

$$q(\xi, s) = [\Psi(\xi, s)]^{1/2} exp[i\phi(\xi, s)], \tag{2}$$

where $\Psi(\xi, s)$ is real and has the meaning of envelope function and $\phi(\xi, s)$ is the real phase function. It is assumed that

$$\lim_{s\to\pm\infty} q(\xi, s) = \lim_{s\to\pm\infty}\frac{\partial q}{\partial s} = 0 \;\Rightarrow\; \lim_{s\to\pm\infty}\Psi(\xi, s) = \lim_{s\to\pm\infty}\frac{\partial \Psi}{\partial s} = 0. \tag{3}$$

Using Equation (2) in Eq. (1), we get

$$\frac{\partial \Psi}{\partial \xi} - \frac{\partial}{\partial s}\left(\Psi\frac{\partial \phi}{\partial s}\right) = 0; \tag{4}$$

$$\frac{1}{4\Psi}\frac{\partial^2\Psi}{\partial\, s^2} - \frac{1}{8\Psi^2}\left(\frac{\partial\Psi}{\partial\, s}\right)^2 - \frac{\Psi}{1+\gamma\Psi} = -\frac{\partial\phi}{\partial\xi} + \frac{1}{2}\left(\frac{\partial\phi}{\partial s}\right)^2. \tag{5}$$

For the profile to be undistorted, we require $\partial\Psi/\partial\xi = 0$, so that from (4) we have

$$\Psi\,(s)\,\frac{\partial\,\phi\,(\xi, s)}{\partial\, s} = C\,(\xi, s)\,. \tag{6}$$

The stationary/locality conditions in ξ require $C(\xi,\, s) = 0$ to yield

$$\frac{\partial\phi\,(\xi, s)}{\partial s} = 0, \tag{6a}$$

since $\Psi(s) \neq 0$. And, (5) implies that ϕ is a constant with respect to s, say ϕ_o. Then from the right hand side of (5) one can deduce that

$$-\frac{\partial\phi}{\partial\xi} = -\beta, \tag{6b}$$

from which it is simple to show that

$$\phi(\xi) = \beta\xi + \phi_o \quad \Rightarrow \quad \phi(\xi = 0, s) = \phi_o, \tag{7}$$

where β is a constant and has the meaning of wave-number shift.

From Equations (5) and (7) we derive the first integral:

$$\left(\frac{d\Psi}{ds}\right)^2 = -8\left(\beta - \frac{1}{\gamma}\right)\Psi^2 - \frac{8}{\gamma^2}\Psi\ln\left(1+\gamma\Psi\right). \tag{8}$$

Next, applying initial condition, i.e., $\Psi(s = 0) \equiv \quad \Psi_o$ = constant, and boundary conditions from Equations (3), to Equation (8), we get

$$\beta = \frac{1}{\gamma}\left\{1 - \frac{\ln\left(1+y_o\right)}{y_o}\right\}, \tag{9}$$

$$\frac{dy}{ds} = \frac{2y}{\gamma^{1/2}}\left\{\frac{\ln\left(1+y\right)}{y} - \frac{\ln\left(1+y_o\right)}{y_o}\right\}^{1/2}, \tag{10}$$

where $y = \gamma\Psi$ and $\mathrm{y}_o = \gamma\Psi_o$,i.e.,$\Psi_o$ implies the dimensionless input intensity. One can see from Equation (9) that the input intensity determines β.

The first order ordinary differential Equation (10) can be written as

$$s - s_o = \frac{\gamma^{1/2}}{2}\int_y^{y_o}\frac{1}{y}\left\{\frac{\ln(1+y)}{y} - C_o\right\}^{-1/2} dy, \tag{11}$$

where

$$C_o = \frac{\ln(1+y_o)}{y_o}, \tag{12}$$

and s_o defines centre of the soliton, usually taken to be 0.

Equations (10) and (11) are equivalent and lead to alternative algorithms for the stationary profiles. As an unsolved intermediate problem of mathematics, it is challenging to note that Equations (10) and (11) are not integrable in the sense of working out a closed form expression for y.

3. The numerical schemes

There are two main successively related stages for the schemes. First is the generation of the initial pulse. Data obtained were then regenerated by linear interpolation and used for the second stage, i.e. an explicit finite-difference scheme.

Values of Ψ_o and γ were chosen as follows. The saturation parameter is measured from $\gamma = I_o/I_s$, where I_s, the saturation intensity of the fibre, is experimentally obtainable. Typically, a Schott OG glass fibre has saturation intensity of $\sim 2.2 \times 10^{22}$ W/m^2. If we need to model a fibre with $\gamma = 0.45$, the input intensity needed from a laser source will be $I_o \sim 9.9 \times 10^{21}$ W/m^2. If the fibre's cross-sectional area is 10 μm^2, the input field will be $A_o \sim 7.45/n_o \times 10^{14}$ V. However, as mentioned in the introduction, a saturable optical fibre supports the phenomena of a two-state solution, whereas one finds that one value of saturation parameter supports two different profiles, corresponding to two maximum dimensionless amplitudes [9, 10]. The lower-state value will have 1.0 unit of maximum dimensionless amplitude as in the case of CNLSE. But, the upper-state value is normally greater than 1.0 unit. The characteristic features of the soliton pulse in the latter case differs for a fundamental soliton and even more so for higher order solitons. In order to observe such peculiar features, we chose $\Psi_o > 1.0$ unit.

3.1. Generation of initial pulse

For given values of Ψ_o and γ, values of y_o and β were calculated. We then numerically integrated Equation (11) using the (142 ... 241) Simpson's rule. The maximum amplitude of the fundamental soliton is given by $|q_o| = (y_o/\gamma)^{1/2}$. Figure 1 shows the corresponding input pulse profiles calculated from Eq. (11) for two values of γ.

Simpson's rule uses uniformly spaced values of y so the values of s that are obtained are not uniformly spaced. However, they are sufficiently close that linear interpolation is adequate to produce the uniform s mesh that is required for the finite-difference simulation.

3.2. Forward-difference and central-difference

We used a combination of the forward-difference and central-difference approximations for the derivative terms of Equation (1) to obtain soliton pulse evolutions. For fundamental soliton pulse dynamics, the net equations of the forward-difference and central-difference schemes are respectively given by

$$q_m^{n+1} = q_m^n + \frac{i\Delta\xi}{2(\Delta s)^2}\left(q_{m+1}^n - 2q_m^n + q_{m-1}^n\right) + \frac{i\Delta\xi|q_m^n|^2 q_m^n}{1+\gamma|q_m^n|^2}, \tag{13}$$

$$q_m^{n+1} = q_m^{n-1} + \frac{i\Delta\xi}{(\Delta s)^2}\left(q_{m+1}^n - 2q_m^n + q_{m-1}^n\right) + \frac{2i\Delta\xi|q_m^n|^2 q_m^n}{1+\gamma|q_m^n|^2}, \tag{14}$$

where m is the mesh index along the dimensionless time axis (s), n indexes the meshes for the dimensionless distance ξ of pulse evolution, and Δs and $\Delta\xi$ are the respective mesh sizes. Values of m were in the range $-M$ to $+M$ with $M = 200$. The periodic grid boundary condition of the form $q(M) = q(-M)$ was used in order to reduce the s range, saving computational time.

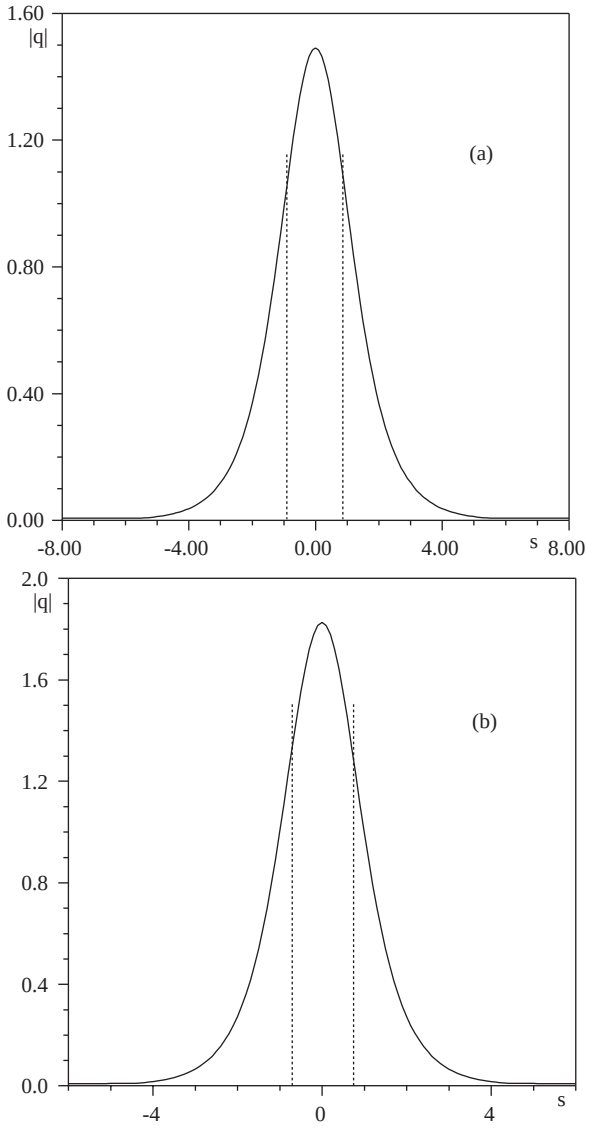

Figure 1. Localized pulse profiles: (a) $|q_o| \cong 1.4907$ units, $\gamma = 0.45$, (b) $|q_o| = 1.8274$ units, $\gamma = 0.3$. Vertical lines indicate the full width at half of maximum intensity, FWHM.

Following [6], our procedure was as follows. The simulation began with the forward-difference for the first ξ step. The step size is chosen as $\Delta\xi = 0.003$ and subsequently used to propagate the pulse along ξ. However, this size is too big for the forward-difference owing to its numerical instability. A smaller value of $\Delta\xi = 0.003/600$ was thus used to gain stability and accuracy. For subsequent ξ-steps, the more stable central-difference scheme was used. As seen from (14) this scheme needs two initial sets of values and these were readily supplied using the initial pulse data profile and the forward-difference scheme for which $\xi = 0.003$. We should note that the s mesh was 0.1 and found no effect if $\Delta s < 0.1$.

The standard conservation laws of Eq. (1) yield three conserved quantities as follows [6, 13]:

$$I_o = \int_{-\infty}^{+\infty} |\, q|^2 ds \tag{15}$$

$$I_1 = \int_{-\infty}^{+\infty} \left\{ \frac{1}{\gamma} |\, q\,|^2 - \left| \frac{\partial q}{\partial s} \right|^2 - \frac{1}{\gamma^2} \ln\left(1 + \gamma\, |\, q\,|^2 \right) \right\} ds \tag{16}$$

$$I_2 = i \int_{-\infty}^{+\infty} \left(q \frac{\partial q^*}{\partial s} - q^* \frac{\partial q}{\partial s} \right) ds, \tag{17}$$

where the asterisk denotes complex conjugate. Both the forward- and the central-difference satisfy the conservation laws, namely $I_o = I_1 = I_2 =$ constant. As mentioned in the introduction, calculation of these conserved quantities provides an efficient tool for checking numerical accuracy and they are easily calculated. Here, the numerical checking was carried out at each $\Delta\xi$ step. Further discussion on this is presented in the next section.

4. Discussion of Numerical Results

Numerical results for propagation of the fundamental and second order solitons corresponding to the pulse profiles of Figures 1a and 1b are shown in Figure 2. As discussed in the previous section, convergence was checked by means of the conserved quantity Equations (15)–(17). Physically, these equations signify particle or photon number, pulse energy and momentum, respectively. The first two conserved quantities suffice as a reliable test of convergence [12]. Numerical accuracy arising from the use of the conserved quantities is simple to observe in the simulations of fundamental solitons depicted by Figures 2a, and 2c, respectively, but not so obvious in simulations of the higher order solitons. The reason is that the higher order solitons possess inherent periodic structures which become increasingly complex as the order increases [5, 14]. Figures 2b, and 2d depict simulations of typical second order soliton pulse propagating in saturable optical fibres.

In simulating the fundamental solitons (refer to Figures 2a and 2c) values of $|\Delta I_o/I_o|$ and $|\Delta I_1/I_1|$ were calculated. The minimum and maximum values of the former differ by much less than 0.5%. However, the maximum value of $|\Delta I_1/I_1|$ is found to be $\approx$1.25%, while the minimum is much less than 0.1%. The comparatively large differences in minimum and maximum values of $\mathrm{I_1}$ may be attributable to its sensitivity to numerical accuracy [12], achieved as the dimensionless distance ξ increases. Further test of convergence, agreeing with our estimated $|\Delta I_o/I_o|$, is confirmed by observing that at the dimensionless distances of 3.00 and 6.00 the pulse profile remains practically undistorted.

Higher order solitons can be simulated if the input pulse is given as

$$q\,(N,\, s,\, \xi = 0) = N\, q\,(s)\,, \tag{18}$$

where $q(s)$ corresponds to the interpolated values for the fundamental stationary profile, and $N = \tau_o \mathrm{A}_o (k_o n_2 / |\beta_2|)^{1/2}$ denotes the soliton order and N is an integer ($N = 1, 2, 3, 4, \ldots$). The higher order solitons do not maintain their shape with propagation but change shape in a periodic manner. Figures 2b and 2d illustrate the case for $N = 2$, the second order soliton pulse.

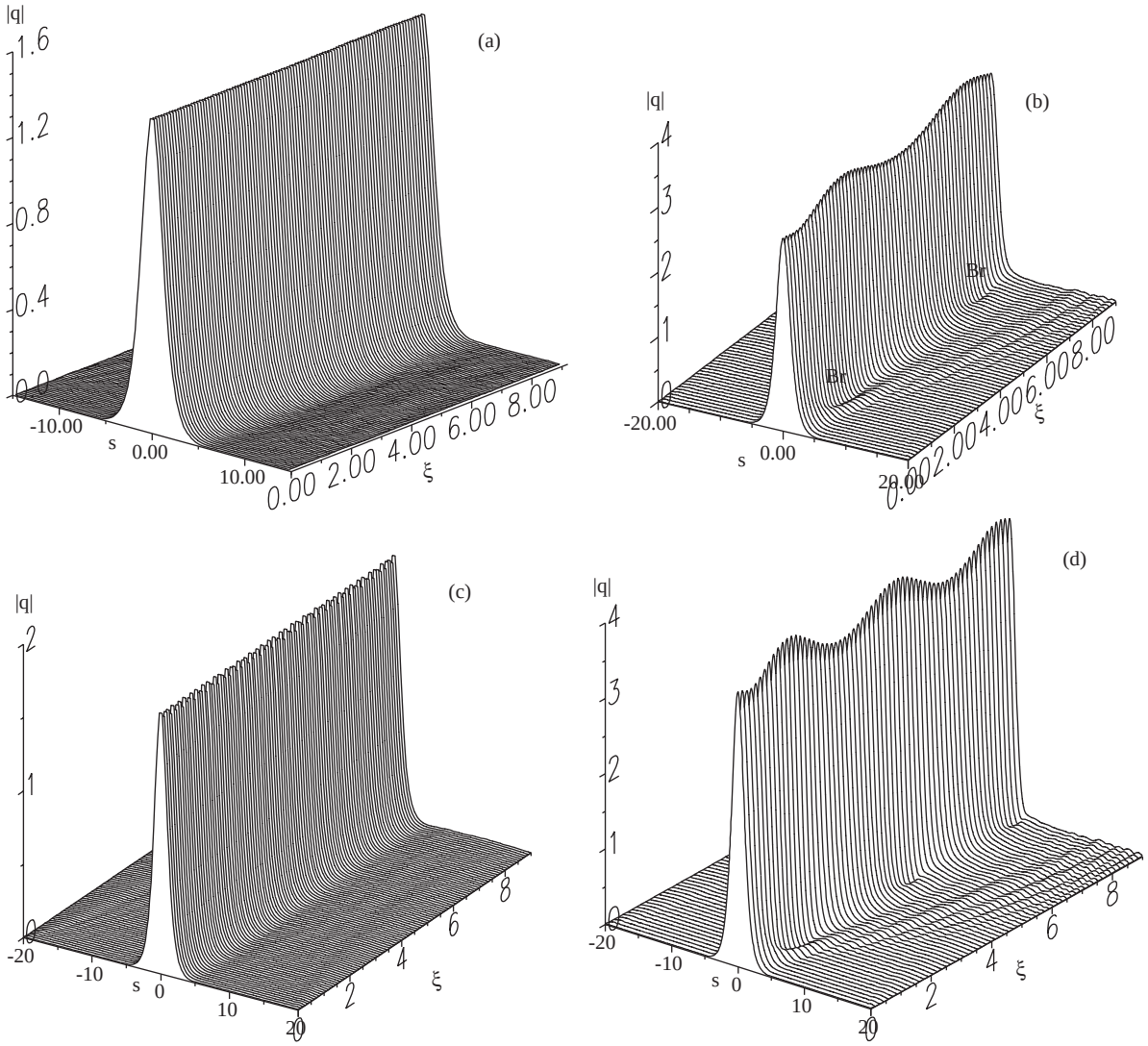

Figure 2. Dynamical pulse profiles: (a) fundamental soliton pulse propagation using input pulse of Figure 1a; (b) second order soliton propagation using input pulse profile of Figure 1a; (c) fundamental soliton using input pulse of Figure 1b; and (d) second order soliton using the pulse profile of Figure 1b.

Two features are observed in the simulations (see Figures 2b and 2d). First is the regular reappearance or the periodic structure of the input pulse. This gives an indication of the soliton period defined as the distance over which higher-order soliton pulses repeat their profiles. The soliton period z_o is given by [4]

$$z_o = \frac{\pi}{2} L_D = \frac{\pi}{2} \frac{\tau_o^2}{|\beta_2|} = 0.322 \frac{\pi}{2} \frac{\tau_{FWHM}^2}{|\beta_2|}, \tag{19}$$

where $\tau_{FWHM} = 1.76\tau_o$, (see Figure 3). Secondly, the simulations show a breathing feature which is also periodic. The breathing feature appears as oscillations at the base of pulse tail, denoted as B_r in Figure 2b.

As seen in Figure 3, the input pulse reappears after a propagation distance of AB. This means that the conserved quantities are applicable for checking numerical accuracy. We calculated the two conserved quantities by tracking the periodic reappearance of the input pulse. We found that the values of $|\Delta I_o/I_o|$ and $|\Delta I_1/I_1|$ are the same as those for the fundamental soliton simulations.

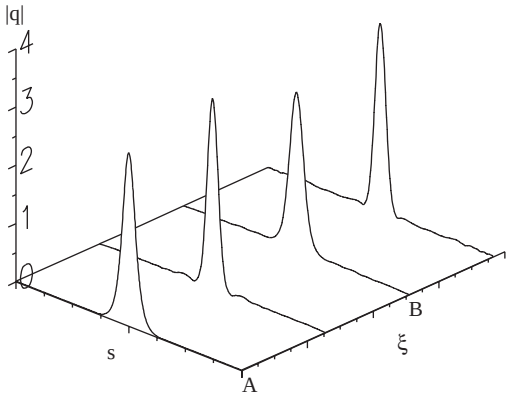

Figure 3. Dynamic second order soliton showing periodic features of Figures 2b and 2d. The distance over which input pulse reappears is AB = 4.35 units.

5. Conclusions

We have demonstrated how soliton pulse propagation in a saturable optical fibre can be simulated using a simple finite-difference scheme. We have also shown that the numerical scheme we used provides similar accuracy as the pseudospectral method and it has an added advantage of providing an easy way of checking the numerical accuracy through calculating the conserved quantities of the governing equation.

Acknowledgement

A. Usman is grateful to the MTCP/JPA of Malaysian Government for financial support during his PhD study at Universiti Sains Malaysia (USM).

References

[1] N. Doran and B. Ian, *Physics World*, **9**, (1996), 35.

[2] C. Sabih and M. Pual, *Phys. Educ.* **35**, (2000), 226.

[3] D. Emmanuel, *Physics Today*, **47**, (2000), 20.

[4] G.P. Agrawal, *Nonlinear Fiber Optics*, (Academic Press, London, 1989).

[5] K.J. Blow and N. Doran, *Nonlinear propagation effects in optical fibers: numerical studies*, in *Optical Solitons — Theory and Experiment*, ed. J. R. Taylor, (Cambridge, 1992), 73.

[6] A. Usman, Ph.D Thesis, School of Physics, University of Science, Malaysia, (USM), 2000.

[7] A. Usman, J. Osman and D.R. Tilley, *J. Nonlin. Opt. Phys. Mater.*, **7**, (1998), 461.

[8] A. Usman and J. Osman, *Telekom Malaysia*, **11**, (1999), 30.

[9] A. Kumar, T. Kurtz and W. Lauterborn, *Phys. Rev. E*, **53**, (1996), 1166.

[10] S. Gatz and J. Hermann, *J. Opt. Soc. Am. B*, **8**, (1991), 2296.

[11] A. Usman, J. Osman and D.R. Tilley, *J. Phys. A: Math. Gen.*, **31**, (1998), 8397.

[12] C. Sturt, R.H. Enns, S.S. Rangnekar and S. S. Sukhpal, *Can. J. Phys.*, **64**, (1986), 311.

[13] M. Delfour, M. Fortin, and G. Payre, *J. Comput. Phys.* **44**, (1981), 277.

[14] N. Doran and K.J. Blow, *IEEE J. Quantum Electron.*, QE-**19**, (1983), 1883.